

Collagen metabolic disorder induced by oxidative stress in human uterosacral ligament-derived fibroblasts: A possible pathophysiological mechanism in pelvic organ prolapse

CHENG LIU*, QING YANG*, GUI FANG, BING-SHU LI, DE-BIN WU,
WEN-JUN GUO, SHA-SHA HONG and LI HONG

Department of Gynecology and Obstetrics, Renmin Hospital of Wuhan University, Wuhan, Hubei 430060, P.R. China

Received March 18, 2015; Accepted January 20, 2016

DOI: 10.3892/mmr.2016.4919

Abstract. Pelvic organ prolapse (POP) is a global health problem, for which the pathophysiological mechanism remains to be fully elucidated. The loss of extracellular matrix protein has been considered to be the most important molecular basis facilitating the development of POP. Oxidative stress (OS) is a well-recognized mechanism involved in fiber metabolic disorders. The present study aimed to clarify whether OS exists in the uterosacral ligament (USL) with POP, and to investigate the precise role of OS in collagen metabolism in human USL fibroblasts (hUSLFs). In the present study, 8-hydroxyguanosine (8-OHdG) and 4-hydroxynonenal (4-HNE), as oxidative biomarkers, were examined by immunohistochemistry to evaluate oxidative injury in USL sections in POP (n=20) and non-POP (n=20) groups. The primary cultured hUSLFs were treated with exogenous H₂O₂ to establish an original OS cell model, in which the expression levels of collagen, type 1, α 1 (COL1A1), matrix metalloproteinase (MMP)-2, tissue inhibitor of metalloproteinase (TIMP)-2 and transforming growth factor (TGF)- β 1 were evaluated by western blot and reverse transcription-quantitative polymerase chain reaction analyses. The results showed that the expression levels of 8-OHdG and 4-HNE in the POP group were significantly higher, compared with those in the control group. Collagen metabolism was regulated by H₂O₂ exposure in a concentration-dependent manner, in which lower concentrations of H₂O₂ (0.1-0.2 mM) stimulated the anabolism of COL1A1, whereas a higher concentration (0.4 mM) promoted catabolism. The expression

levels of MMP-2, TIMP-2 and TGF- β 1 exhibited corresponding changes with the OS levels. These results suggested that OS may be involved in the pathophysiology of POP by contributing to collagen metabolic disorder in a severity-dependent manner in hUSLFs, possibly through the regulation of MMPs, TIMPs and TGF- β 1 indirectly.

Introduction

Pelvic organ prolapse (POP) is a global health problem, which adversely affects 50% of women >50 years old, in terms of poor life quality and increasing economic burden (1-3), and has become one of the most common indications for gynecological surgery in elderly women (4). However, the etiology and pathophysiological mechanisms remain to be fully elucidated. POP is considered to be a multifactorial etiological disease (5,6). Aging and vaginal childbirth are well established risk factors, and other factors, including obesity, chronic constipation and declined hormonal status (menopause), have also been reported to be associated with prolapse (6). Previous studies have demonstrated pelvic muscle injuries (7), loss of extracellular matrix (ECM) (8-10) and hyperfunction of matrix metalloproteinases (MMPs) (11,12), together with upregulated cell apoptosis and downregulated proliferation in pelvic connective tissue in women with POP (13). The loss of ECM proteins is considered to be the molecular basis facilitating the incidence and development of POP (10).

OS reflects a status of imbalance, in which excessive accumulated reactive oxygen species (ROS) exceeds the neutralizing ability of the redox system in cells, resulting in oxidative damage to cell organisms, including deoxyribonucleic acid (DNA), proteins and lipids. In addition, ROS act as cellular messengers modulating specific signaling pathways (14). Previous studies have suggested that OS is involved in cardiovascular remodeling and fibrotic disorders by activating MMPs, and reducing collagen synthesis in fibroblasts and smooth muscle cells (15-17). Thus, the present study hypothesized that OS may contribute to collagen metabolic disorder in the pathogenesis of POP. If this is the case, it may assist in developing novel clinic therapeutic strategies.

Correspondence to: Dr Li Hong, Department of Gynecology and Obstetrics, Renmin Hospital of Wuhan University, 238 Jiefang Road, Wuhan, Hubei 430060, P.R. China
E-mail: 2013103020057@whu.edu.cn

*Contributed equally

Key words: pelvic organ prolapse, oxidative stress, tissue inhibitor of metalloproteinase, matrix metalloproteinase, collagen metabolism, transforming growth factor- β 1

In the present study, this hypothesis was tested through a number of experiments. Preliminarily, specimens of human uterosacral ligament (USL) were collected to identify the oxidative damage, and assess whether there are differences between women with and without POP. Furthermore, the cytotoxic effect of hydrogen peroxide (H_2O_2) on fibroblasts derived from normal human USL tissues was evaluated. A cell model was also established to mimic intracellular OS, in order to investigate the exact role of OS in collagen metabolism and the associated mechanisms.

Materials and methods

Patient grouping and sample collection. The study was approved by the ethics committee of Renmin Hospital of Wuhan University (Wuhan, China), and each participant provided written informed consent, according to the Declaration of Helsinki (18). A total of 56 menopausal women were enrolled from the Department of Obstetrics and Gynecology, Renmin Hospital of Wuhan University between March 2011 and June 2013. Menopause was defined as the cessation of menses for at least 1 year. The study group consisted of 20 women, who underwent hysterectomy as part of pelvic reconstruction surgery for POP stage II, III or IV, according to POP quantitative examination (POP-Q) (19). In addition, 20 women without POP (non-POP group), who underwent hysterectomy for benign indications, including cervical intraepithelial neoplasia and dysfunctional uterine bleeding, served as the control group. Another 16 non-POP cases were used to develop primary and passage cultures of human uterosacral ligament fibroblasts (hUSLFs). In order to minimize the effects of confounding factors on the expression of OS biomarkers, women who had pelvic infectious diseases, leiomyoma, adenomyosis, endometriosis, history of pelvic surgery, malignant gynecological tumors, systemic autoimmune diseases, cardiovascular diseases, diabetes mellitus or other endocrine disorders, and neuromuscular degenerative diseases were excluded from either group. In addition, women who received hormone replacement therapy or antioxidant supplementation were not included in either group.

Tissue sample biopsies measuring 0.5x1.0 cm were obtained from the USL, close to the cervix, during surgery, following which the specimens were prepared according to the respective following protocols for the different investigations.

Immunohistochemistry. The tissue specimens were fixed with 4% paraformaldehyde and embedded in paraffin (both purchased from Maxim Biotechnology Development Co., Ltd., Fuzhou, China), and then sliced into 4 μ m sections for immunohistochemical staining. An Elivision™ super HRP IHC kit (cat. no. Kit-9921; Fuzhou Maxim Biotechnology Development Co., Ltd.), was used for immunohistochemistry. The paraffin-embedded sections were incubated for 30 min at 60°C, and then deparaffinized and rehydrated in a graded alcohol series. Antigen retrieval was performed by heat mediation in citrate buffer (pH<6) or EDTA buffer (pH>9), according to the product datasheets for the primary antibodies. The sections were then incubated with 3% H_2O_2 (Maxim Biotechnology Development Co., Ltd.) for 10 min

at room temperature to inactivate endogenous peroxidase, and blocked with 5% goat serum for 15 min. The sections were then incubated with primary antibodies overnight at 4°C. Following incubation with streptavidin peroxidase (Maxim Biotechnology Development Co., Ltd.) for 10 min at room temperature, secondary antibodies were added for 30 min at 37°C. The immune reaction was then visualized using DAB (Fuzhou Maxim Biotechnology Development Co., Ltd., Fuzhou, China). The specimens were washed with phosphate-buffered saline (PBS) following each step in the protocol. For the negative controls, the primary antibody was replaced with PBS. The following antibodies were used: Mouse monoclonal anti-8-hydroxyguanosine (8-OHdG) antibody (1:100 dilution; ab62623; Abcam, Cambridge, UK), rabbit polyclonal anti-4-hydroxynonenal (4-HNE) antibody (1:200 dilution; ab46545; Abcam) and rabbit polyclonal anti-TGF- β 1 antibody (1:100 dilution; ab53169; Abcam). Secondary antibodies included goat anti-rabbit polyclonal horseradish peroxidase (HRP)-conjugated IgG (1:1,000 dilution; ab97051; Abcam) and goat anti-mouse polyclonal HRP-conjugated IgG (1:1,000 dilution; ab97023; Abcam). Immunoreactivity was quantified by the integrated optical density value, obtained from immunohistochemical images using Image-Pro Plus 6.0 software.

Primary cell culture and passaging. hUSLFs were developed from the fresh USL biopsy tissues, according to Gibco (Thermo Fisher Scientific, Inc., Waltham, MA, USA) protocols for primary culture. Briefly, the tissue samples were cut into small sections (~1 mm³) and washed twice in PBS, followed by digestion with collagenase I (Invitrogen; Thermo Fisher Scientific, Inc.) and trypsin (Sigma-Aldrich, St. Louis, MO, USA) successively. The isolated cells were routinely cultured in Dulbecco's modified Eagle's medium (GE Healthcare Life Sciences, Logan, UT, USA) supplemented with 10% fetal bovine serum, 1% penicillin (100 U/ml) and streptomycin (100 μ g/ml) (Gibco; Thermo Fisher Scientific, Inc.) in a 5% CO₂-humidified atmosphere at 37°C. The cells were subcultured at a confluence of 80%. To identify the cells as fibroblasts, immunocytochemical analyses were performed. Cytokeratin is a specific biomarker for epithelial original cells, while vimentin is a specific biomarker for mesenchymal original cells (20). Cells were seeded into a six-well plate containing a pre-placed coverslip at a density of 1x10⁵ cells/ml, and incubated at 37°C for 48 h. The cells were harvested at 70% confluence, washed with PBS and fixed in 4% paraformaldehyde for 20 min at room temperature, and then permeabilized using 0.3% Triton X100 buffer (Sigma-Aldrich) for 10 min at room temperature. After three washes with PBS, the cells were incubated with 3% H_2O_2 for 10 min at room temperature to inactivate the endogenous peroxidase. After being washed thrice with PBS, the slides were blocked with 1% bovine serum albumin (Sigma-Aldrich) in PBS for 30 min at room temperature. Next, the cells were incubated with mouse monoclonal vimentin (1:200 dilution; sc6260; Santa Cruz Biotechnology, Inc., Santa Cruz, CA, USA), and mouse monoclonal cytokeratin-19 (1:200 dilution; sc6278; Santa Cruz Biotechnology, Inc.) antibodies overnight at 4°C followed by three washes in PBS. Subsequently, the cells were incubated with secondary antibodies (k5007; Dako, Glostrup, Denmark) at room temperature for 1 h followed by three washes in PBS,

and visualized using 3,3'-diaminobenzidine (k5007; Dako). The immunocytochemical staining slides were evaluated using a microscope (BX51; Olympus Corporation, Tokyo, Japan).

Cell Counting Kit-8 (CCK-8) assay for assessment of cytotoxicity. Cytotoxicity was measured using a CCK-8 assay (Beyotime Institute of Biotechnology, Haimen, China). Cells suspended with Dulbecco's modified Eagle medium (100 μ l; Gibco; Thermo Fisher Scientific) were inoculated into a 96-well plate (5,000 cells/well) and incubated for 24 h at 37°C, following which the spent culture medium was removed and 100 μ l of prepared media containing various concentrations of H₂O₂ (0, 0.2, 0.4, 0.8 and 1.6 mM) was added. Each sample was loaded in triplicate. Following incubation at 37°C for 4 and 24 h respectively, 10 μ l CCK-8 solution was added into each well and incubated at 37°C for 4 h. The absorbance was measured at 450 nm using a microplate spectrophotometer (Victor3 1420 Multilable Counter; PerkinElmer, Inc., Waltham, MA, USA). The viability of the treated group was expressed as a percentage of the untreated control group, which was designated as 100%.

Flowcytometric assay for cell apoptosis. Annexin V-fluorescein isothiocyanate (FITC)/propidium iodide (PI) double staining was used to assay cell apoptosis, in strict accordance with the manufacturer's protocols (Beyotime Institute of Biotechnology). In brief, the cells were resuspended at a density of 1x10⁶/ml and incubated with 10 μ l Annexin V-FITC at room temperature for 30 min in the dark. Subsequently, 5 μ l PI was added for 5 min, following which 400 μ l 1X binding buffer was added into each tube. A flow cytometer (BD FACSCalibur; BD Biosciences, San Jose, CA, USA) was finally used to detect the labeled cells.

Direct immunofluorescent assay for intracellular ROS. Following exposure to different concentrations of H₂O₂, The cells were incubated with 10 μ M 2',7'-dichlorofluorescein diacetate (DCF-DA; Applygen Technologies, Inc., Beijing, China), a peroxide sensitive fluorescent probe, for 30 min at 37°C, according to the manufacturer's protocol. Images were captured with a fluorescent microscope (BC51; Olympus Corporation) and analyzed using Image-pro Plus 6.0 software (Media Cybernetics, Inc., Rockville, MD, USA).

Indirect immunofluorescent assay for intracellular 8-OHdG. Following treatment with H₂O₂ solution or the placebo, the plated cells were fixed and incubated with mouse monoclonal anti-8-OHdG (1:100 dilution; ab62623; Abcam) overnight at 4°C, and were then successively incubated with fluorescent-labeled goat anti-mouse polyclonal IgG secondary antibody (1:500 dilution; ab150117; Abcam) and DAPI (2 μ g/ml; Beyotime Institute of Biotechnology) at room temperature for 20 min, according to routine protocols. The cells were observed under a fluorescent microscope (Olympus Corporation) and analyzed using Image-pro Plus 6.0 software.

Western blot analysis. Total protein was extracted from the USL cells using radioimmunoprecipitation assay buffer (Beyotime Institute of Biotechnology) containing phenylmethylsulfonyl fluoride, and the quantity was determined using a Bicinchoninic

Acid Protein Assay kit (Beyotime Institute of Biotechnology). The protein samples (20 μ g) were separated by electrophoresis on SDS-PAGE gels (10%; Beyotime Institute of Biotechnology) and transferred onto polyvinylidene fluoride (PVDF) membranes (EMD Millipore, Billerica, MA, USA). Following blocking, the membranes were incubated overnight at 4°C with diluted primary antibody. The PVDF membranes were then washed three times with Tris-buffered saline with 0.1% Tween 20 (Beyotime Institute of Biotechnology), and the blots were incubated with IRDye 800CW goat anti-rabbit/mouse secondary antibodies (1:10,000 dilution; LI-COR Biosciences, Lincoln, NE, USA) at room temperature for 1 h. Finally, the protein intensity were scanned as a fluorescent signal and quantified using an Odyssey imaging system (LI-COR Biosciences, Lincoln, NE, USA). Experiments were performed in triplicate. The following primary antibodies were used: Polyclonal rabbit collagen, type 1, α 1 (COL1A1) antibody (1:400 dilution, sc-8784-R), polyclonal rabbit MMP-2 antibody (1:400 dilution; sc-10736), polyclonal rabbit TIMP-2 antibody (1:500 dilution; sc-5539) (all purchased from Santa Cruz Biotechnology, Inc.) and polyclonal rabbit TGF- β 1 antibody (1:1,000 dilution; ab53169; Abcam). GAPDH antibody (1:1000 dilution; sc-25778; Santa Cruz Biotechnology, Inc.) served as an endogenous reference.

Reverse transcription-quantitative polymerase chain reaction (RT-qPCR) analysis. Total RNA was extracted using TRIzol reagent (Invitrogen; Thermo Fisher Scientific, Inc.), according to the manufacturer's protocol. cDNA synthesis was performed with 2 μ g of total RNA in a reaction volume of 20 μ l using a RevertAid First Strand cDNA Synthesis kit (Fermentas; Thermo Fisher Scientific, Inc.) containing 6 μ l total RNA, 1 μ l oligo 18 primer, 5 μ l diethylpyrocarbonate water, 4 μ l 5X reaction buffer, 1 μ l Ribolock RNase inhibitor, 2 μ l 10 mM dNTP and 1 μ l RevertAid M-MuLV Reverse Transcriptase. SYBR Green labeled probes (Takara Bio, Inc., Tokyo, Japan) were used to detect gene expression levels in an ABI 7500 Real-Time PCR system (Applied Biosystems; Thermo Fisher Scientific, Inc.). The expression levels of the target mRNAs were calculated and normalized to the mRNA level of GAPDH. The following primers (Sangon Biotech Co., Ltd., Shanghai, China) were used: GAPDH (used for normalization), forward 5'-GAAGGTGAAGGTCGGAGTC-3' and reverse 5'-GAA GATGGTGATGGGATTTC-3'; COL1A1, forward 5'-CAA GACGAAGACATCCCACCAATC-3' and reverse 5'-ACA GATCACGTCATCGCACAACA-3'; MMP-2, forward 5'-AGTTTCCATTCCGCTTCCAG-3' and reverse 5'-CGG TCGTAGTCCTCAGTGGT-3'; TIMP-2, forward 5'-TCT GGAAACGACATTTATGG-3' and reverse 5'-GTTGGA GGCCTGCTTATGGG-3'; and TGF- β 1, forward 5'-TAT TGAGCACCTTGGGCACT-3' and reverse 5'-ACCTCTCTG GGCTTGTTTCC-3'. The thermal cycling conditions were as follows: 30 Sec at 95°C, followed by 40 cycles of 5 sec at 95°C and 34 sec at 60°C, and finally 15 sec at 95°C, 1 min at 60°C, 15 sec at 95°C and 15 sec at 60°C. mRNA levels were subsequently quantified using the 2^{- $\Delta\Delta$ C_q} method (21).

Statistical analysis. The experiments were repeated at least three times and data are partially presented as the mean \pm standard

Table I. Demographic and clinical characteristics of all participants.

Parameter	POP group (n=20)	Control group (n=20)	P-value
Age (years)	55.1±4.9	53.6±4.1	NS ^a
Parity	2.2±1.3	1.9±1.1	NS ^a
Body mass index (Kg/m ²)	26.2±5.3	25.2 ±4.9	NS ^a
Postmenopausal duration (months)	58.6±8.9	60.3±9.4	NS ^a

Data are presented as the mean ± standard deviation. ^aNS, no significance at P<0.05 (Mann-Whitney *U* test). POP, pelvic organ prolapse.

deviation. A Mann-Whitney *U* test was used for comparison between two groups, One-way/two-way analysis of variance (ANOVA) was used to analyze the statistical difference among groups. GraphPad Prism 5.01 (GraphPad Software, Inc.) and SPSS 16.0 (SPSS, Inc., Chicago, IL, USA) were used for statistical analyses and graph plotting. P<0.05 was considered to indicate a statistically significant difference.

Results

Demographic and clinical characteristics. All 40 subjects among the two groups were well matched in terms of demographic and clinical characteristics. No significant differences in age, parity, body mass index or postmenopausal duration were observed between the POP group and the control group (Table I).

Expression of OS biomarkers are upregulated in POP USL tissues. Through immunohistochemical investigations, the present study found that the immunoreactivity of 8-OHdG in the POP group was significantly higher, compared with that in the control group (0.625±0.145, vs. 0.263±0.117, respectively; P<0.01). The same results were observed for 4-HNE between the POP and control groups (0.027±0.006, vs. 0.016±0.006, respectively; P<0.01; Fig. 1).

Cytotoxic effects are induced by exogenous H₂O₂ in fibroblasts. To evaluate the cytotoxicity of exogenous H₂O₂ on the hUSLFs, the fibroblasts were treated with graded H₂O₂ at concentrations of 0, 0.1, 0.2, 0.4, 0.6, 0.8 and 1.0 mM for 2, 4, 6, 8, 12 and 24 h, respectively, following which cell viability was examined using a CCK-8 assay. As shown in Fig. 2, cell viability decreased following H₂O₂ treatment in time-dependent and concentration-dependent manner. Based on two-way ANOVA, no statistically significant difference was observed between the 0.1 mM group and the untreated control group. At concentrations >0.2 mM, the cell viability in the treated groups were significantly different from that of the control group (P<0.05; Fig. 2A). Following comparison of the cell viability at 4 h (Fig. 2B) with that of 24 h (Fig. 2C), significant inter-group differences were found among the groups with concentrations of 0.1, 0.2 and 0.4 mM (one-way ANOVA; P<0.05). Additionally, following treatment for 24 h, concentrations ≥0.4 mM led to a significant decrease in cell viability, however, no significant differences were observed at the 0.4, 0.6, 0.8 and 1.0 mM concentrations. The above data suggested that 0.1 mM may

be a sub-toxic dose, which induces no significant cytotoxicity, whereas 0.2 mM is mildly to moderately toxic and concentrations ≥0.4 mM are severely toxic in a treatment duration of 24 h. Immunocytochemical analyses demonstrated that the cells were anti-vimentin-positive and anti-keratin-negative.

Cell apoptosis is induced by H₂O₂ treatment. Based on the results of the above cytotoxicity investigations, the hUSLFs cells were treated for 24 h with H₂O₂ at concentrations ranging between 0.1 and 0.6 mM, to investigate the effects on cell apoptosis. As shown in Fig. 3, as the concentration of H₂O₂ increased, the apoptotic rates increased gradually. No significant difference was observed between the control group and the 0.1, 0.4 or 0.6 mM groups, however, there were significant differences between the 0.2 mM group and the other groups (P<0.05).

Intracellular ROS generation is induced by incubation with H₂O₂. To confirm the increase of intracellular ROS in hUSLFs, a DCF-DA assay was performed following treatment with H₂O₂ at different concentrations ranging between 0 and 0.6 mM for 24 h. As shown in Fig. 4, with increasing concentrations of H₂O₂, the fluorescence intensity of the oxidized DCF, which indicates the induction of intracellular ROS, gradually increased. There were significant differences among all pairs of groups (P<0.05), with the exception of 0.4 and 0.6 mM. These results revealed that H₂O₂ significantly elevated the levels of intracellular ROS in the hUSLFs following 24 h exposure at concentrations ranging between 0 and 0.4 mM.

Production of 8-OHdG is a biomarker of oxidative damage. To clarify the oxidative damage secondary to the increase of intracellular ROS, the production of 8-OHdG was examined using an indirect immunofluorescent assay. As shown in Fig. 5, as the concentration of H₂O₂ increased between 0 and 0.4 mM, the fluorescence intensity of 8-OHdG, a biomarker of oxidative damage, gradually increased, and the intergroup differences were statistically significant (P<0.05).

H₂O₂ treatment regulates collagen metabolism in fibroblasts. In order to clarify the effects of H₂O₂ treatment on collagen metabolism, and determine the potential mechanism, the present study examined the expression levels of COL1A1, MMP-2, TIMP-2 and TGF-β1 by Western blot and RT-qPCR analyses. As shown in Fig. 6A and B), as the concentration of H₂O₂ increased between from 0 and 0.4 mM, the protein

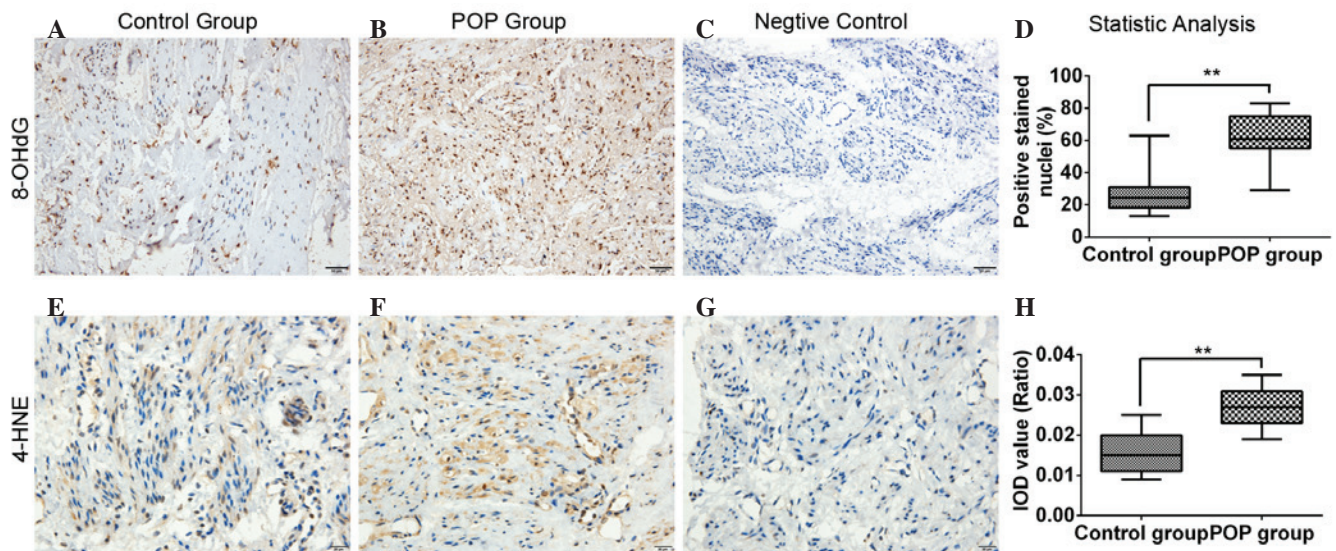


Figure 1. Immunohistochemical analysis for assessment of rgw immunoreactivity of 8-OHdG and 4-HNE in uterosacral ligaments. (A-C) Immunohistochemical staining for 8-OHdG (magnification, x200; scale bar=50 μ m). (D) Statistical analysis, based on the percentage of 8-OHdG-positive stained cells in the total cell count. (E-G) Immunohistochemical staining for 4-HNE (magnification, x400; scale bar=20 μ m). (H) Statistical analysis, based on the IOD value. Data are presented as the mean \pm standard deviation (**P<0.01). 8-OHdG, 8-hydroxyguanosine; 4-HNE, 4-hydroxynonenal; IOD, integrated optical density; POP, pelvic organ prolapse.

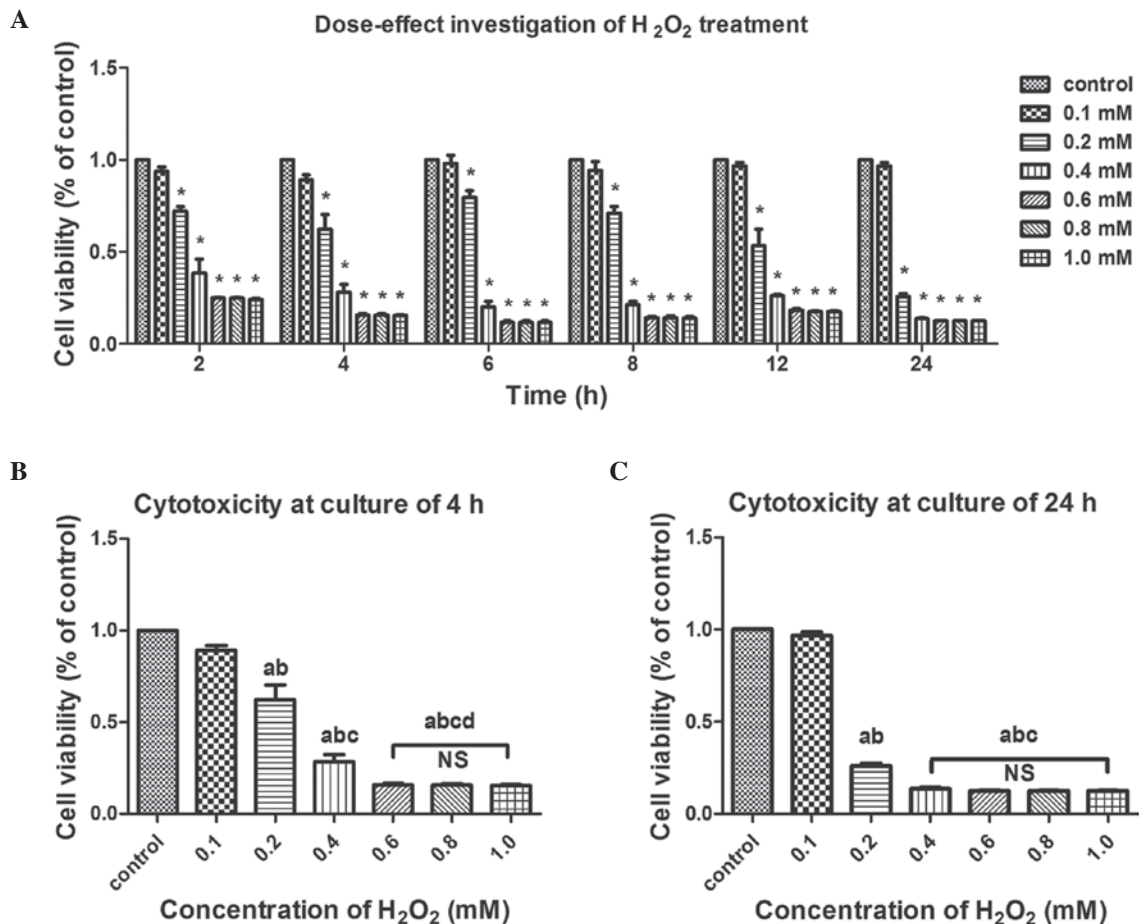


Figure 2. Effects of exogenous H_2O_2 on the cell viability of human uterosacral ligament fibroblasts. Cell viability was examined using a Cell Counting Kit-8 assay and data are presented as a percentage of the untreated control group. (A) Cells were treated with the indicated concentrations of H_2O_2 for 2, 4, 6, 8, 12 and 24 h for determination of concentration-dependence. Cell viability decreased in a concentration-dependent and time-dependent manner under H_2O_2 exposure. *P<0.05, vs. control group (two-way ANOVA). The cells were treated with the indicated concentrations of H_2O_2 for (B) 4 h and (C) 24 h for determination of concentration-dependence. One-way ANOVA was performed, and data are presented as the median \pm standard error of the mean (n=3). a, P<0.05, vs. untreated control; b, P<0.05, vs. 0.1 mM; c, P<0.05, vs. 0.2 mM; d, P<0.05, vs. 0.4 mM; NS, no significance; ANOVA, analysis of variance; H_2O_2 , hydrogen peroxide.

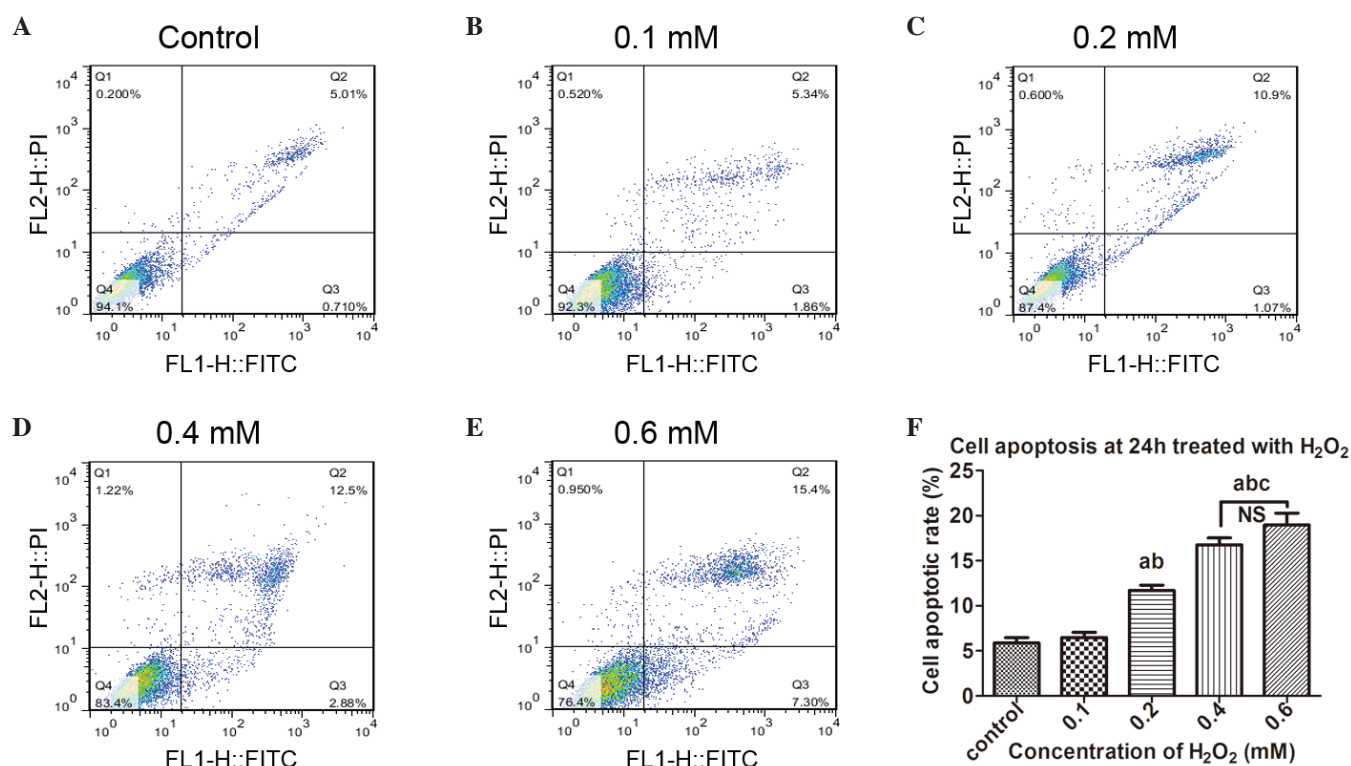


Figure 3. Cell apoptosis is induced by exogenous H_2O_2 . Following treatment with different concentrations of H_2O_2 for 24 h, the human uterosacral ligament fibroblasts were stained with Annexin V/propidium iodide and then assayed using flow cytometry. Cell apoptosis following exposure to (A) 0, (B) 0.1, (C) 0.2, (D) 0.4 and (E) 0.6 mM H_2O_2 . (F) Statistical analysis of the apoptotic rates. Data are presented as the median \pm standard error of the mean (n=3). One-way analysis of variance was performed, followed by an unpaired t-test. Data are presented as the median \pm standard error of the mean (n=3). a, $P < 0.05$, vs. untreated control; b, $P < 0.05$, vs. 0.1 mM; c, $P < 0.05$, vs. 0.2 mM; NS, no significance; H_2O_2 , hydrogen peroxide; PI, propidium iodide; FITC, fluorescein isothiocyanate.

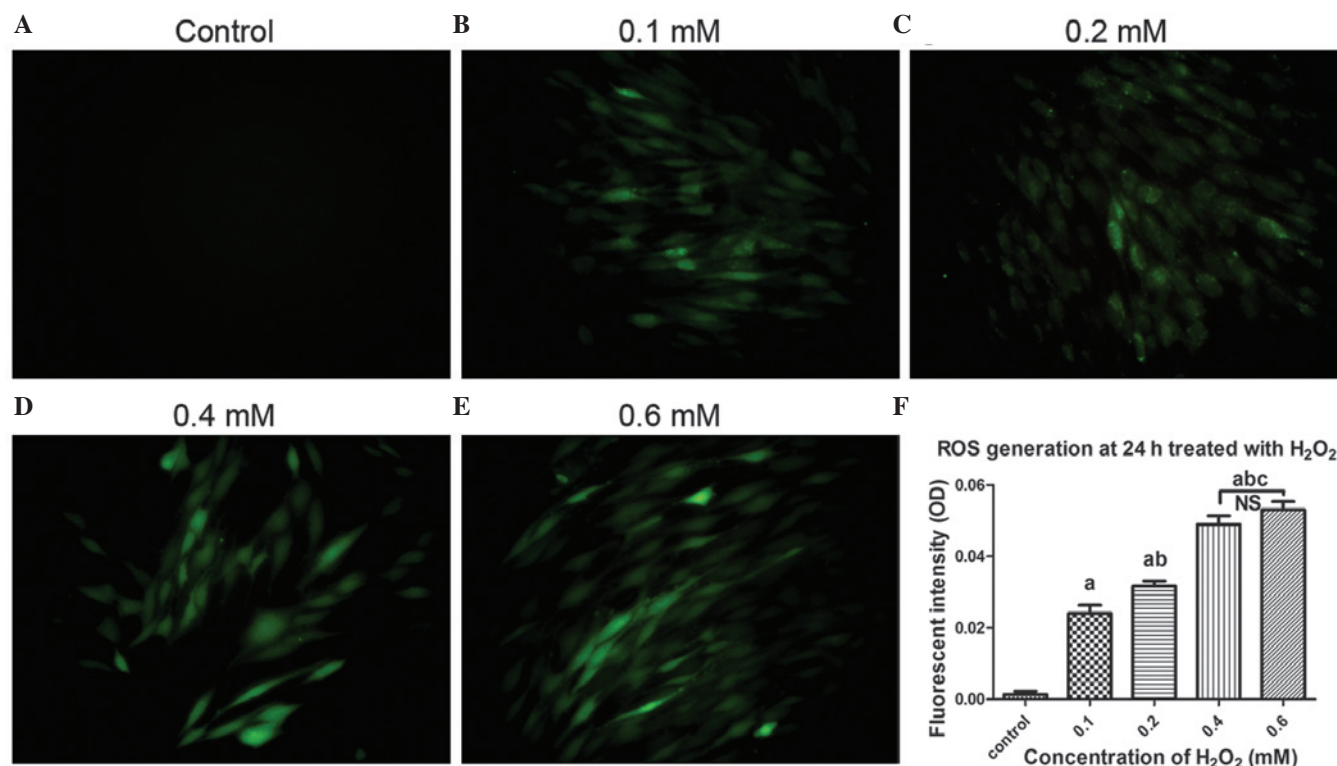


Figure 4. Microscopic images of ROS generation induced by H_2O_2 treatment using DCF-DA staining. The cells were pre-treated with exogenous H_2O_2 at concentrations of (A) 0, (B) 0.1, (C) 0.2, (D) 0.4 and (E) 0.6 mM, and then incubated with DCF-DA. The cells were observed under a fluorescent microscope (magnification, x200). (F) Quantitative analysis based on fluorescence intensity, obtained using Image-pro Plus 6.0 software. Data are presented as the median \pm standard error of the mean. One-way analysis of variance was performed, followed by an unpaired t-test. Data are presented as the median \pm standard error of the mean (n=3). a, $P < 0.05$, vs. untreated control; b, $P < 0.05$, vs. 0.1 mM; c, $P < 0.05$, vs. 0.2 mM; NS, no significance; ROS, reactive oxygen species; OD, optical density; H_2O_2 , hydrogen peroxide; DCF-DA, 2',7'-dichlorofluorescein diacetate.

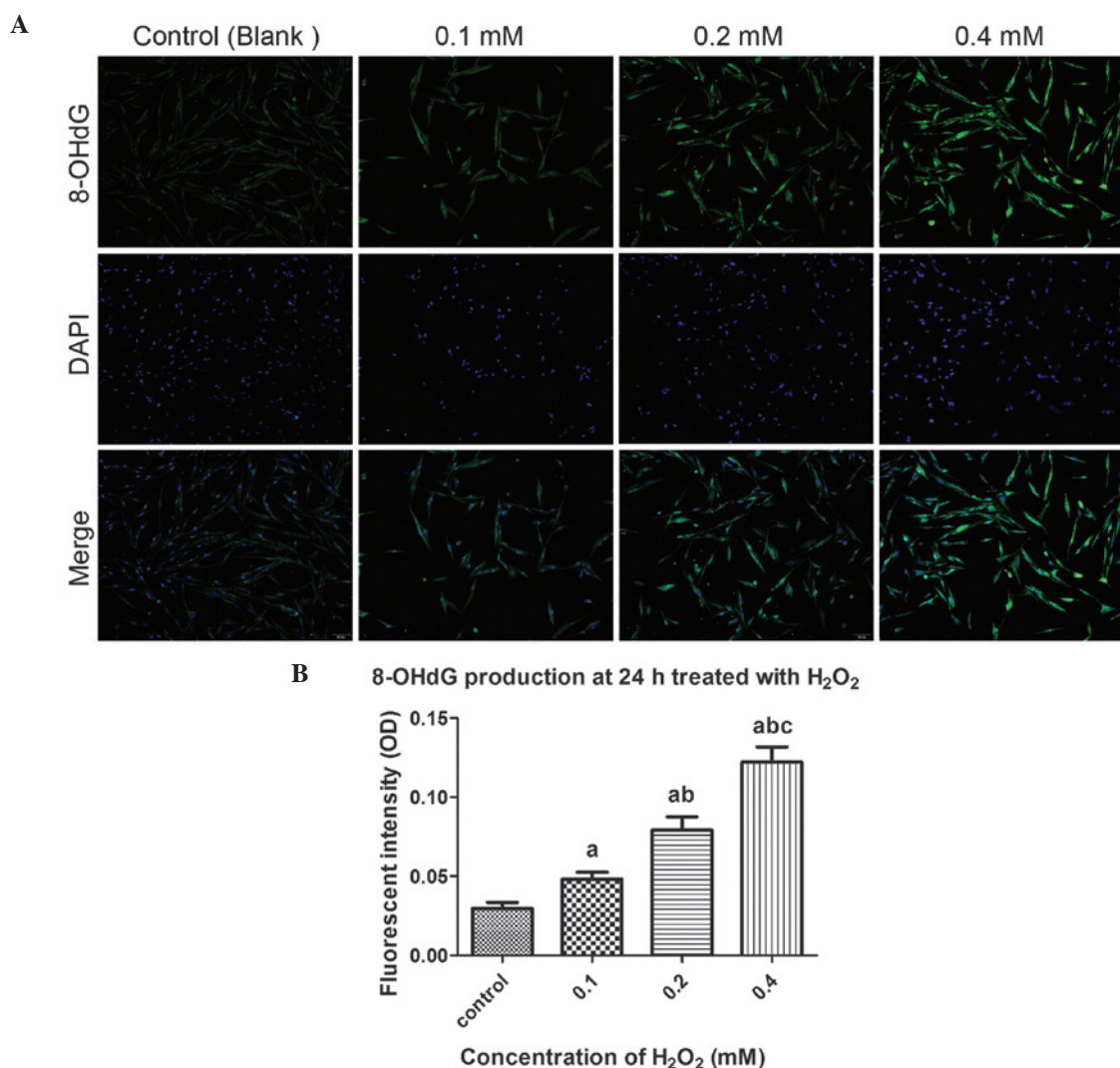


Figure 5. Microscopic images of 8-OHdG production induced by H₂O₂ treatment using an immunofluorescent assay. (A) Cells were pre-treated with exogenous H₂O₂ (0, 0.1, 0.2, and 0.4 mM) for 24 h, followed by incubation with 8-OHdG antibodies and staining with DAPI. The cells were observed under a fluorescent microscope (magnification, x200). (B) Quantitative analysis based on fluorescence intensity, obtained using image-pro plus 6.0 software. One-way analysis of variance was performed, followed by an unpaired t-test. Data are presented as the median \pm standard error of the mean (n=3). a, P<0.05, vs. untreated control; b, P<0.05, vs. 0.1 mM; c, P<0.05, vs. 0.2 mM; NS, no significance; 8-OHdG, 8-hydroxyguanosine; OD, optical density; H₂O₂, hydrogen peroxide.

synthesis of COL1A1 reduced following an initial increase, and the intergroup differences were statistically significant (P<0.05), with the exception of that between the 0.1 and 0.2 mM groups. The protein level of MMP-2 was gradually and significantly increased as the H₂O₂ concentration increased (P<0.05). By contrast, there was a sharp decline in the protein expression of TIMP-2 when the concentration of H₂O₂ increased between 0.1 and 0.4 mM, and the difference among these groups were significant (P<0.05). Notably, TGF- β 1 showed a similar change to that of COL1A1. Based on the RT-qPCR data for COL1A1, MMP-2, TIMP-2 and TGF- β 1 (Fig. 6C-F), it was confirmed that the changes in the mRNA expression levels were consistent with those of the proteins.

Discussion

Previous reports have indicated that metabolic disorder of the ECM, characterized by reduced collagen anabolism and

hyperfunction of MMPs, is the pathological molecular basis of POP (8-12). Aging, vaginal delivery, chronic constipation, obesity and declined hormone status, are well-recognized risk factors (5,6). A number of notable commonalities have been identified regarding the similarities in these risk factors. According to the Free Radical Theory of Aging (22), cell aging is a consequence of oxidative injury in a sense. To recognize the damage to the pelvic floor caused by vaginal delivery, aside from direct trauma at childbirth (23), chronic nerve injuries of the levator ani muscle during pregnancy and postpartum periods have been repeatedly reported (24,25). In addition, obesity and constipation can cause increased intra-abdominal pressure (IAP), which is currently viewed as an exacerbating factor of POP (26), as IAP may exert chronic mechanical strain on the pelvic support structures. *In vitro*, it has been demonstrated that cyclic mechanical stretches cause OS in several types of cell (27-29). Considering these previous findings, the present study hypothesized that OS may mediate the pathogenesis of POP.

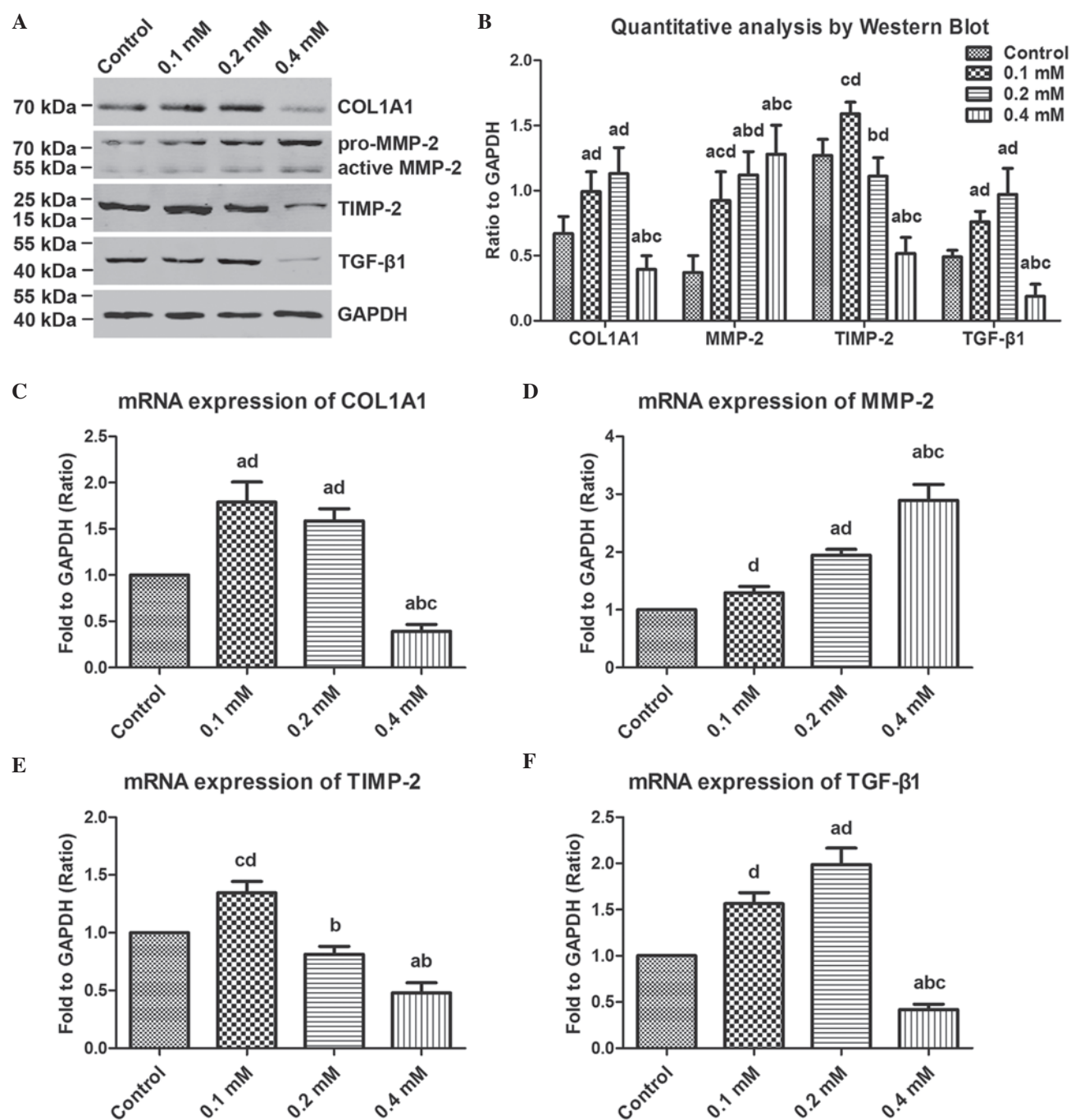


Figure 6. Effects of exogenous H_2O_2 on COL1A1 metabolism in human uterosacral ligament fibroblasts. The cells were pre-treated with the indicated concentrations of H_2O_2 (0, 0.1, 0.2 and 0.4 mM) for 24 h, and then assayed by Western blot and RT-qPCR analyses. (A) COL1A1, MMP-2, TIMP-2 and TGF- β 1 were examined using Western blot analysis at the protein level. (B) Quantitative analysis based on the bands of the Western blot. The mRNA expression levels of (C) COL1A1, (D) MMP-2, (E) TIMP-2 and (F) TGF- β 1 were determined by RT-qPCR. One-way analysis of variance was performed and data are presented as the median \pm standard error of the mean ($n=3$). a, $P<0.05$, vs. untreated control; b, $P<0.05$, vs. 0.1 mM; c, $P<0.05$, vs. 0.2 mM; d, $P<0.05$, vs. 0.4 mM; NS, no significance; COL1A1, collagen, type 1, α 1; MMP-2, matrix metalloproteinase-2; TIMP-2, tissue inhibitor of metalloproteinase-2; TGF- β 1, transforming growth factor- β 1; H_2O_2 , hydrogen peroxide.

According to established experiment design, all participants in the present study were well matched in age, parity, body mass index and postmenopausal duration (Table I), therefore, investigation was performed to confirm whether more serious oxidative injury was present in the women with POP, compared with the normal control group. 8-OHdG is a modified base, which occurs in DNA due to attack by hydroxyl radicals that are formed as by-products and intermediates of aerobic metabolism and during OS (30). 8-OHdG is well correlated

with OS and damage to DNA, which leads to degenerative disease states. As a result, 8-OHdG has become increasingly used as a sensitive, stable and integral marker of oxidative damage in cellular DNA. 4-HNE, as a stable product of lipid peroxidation, has been implicated in the etiology of pathological changes under OS, as a key mediator of OS-induced cell death. Through immunohistochemical examination of USL sections, the present study found significantly high levels of 8-OHdG and 4-HNE immunoreactivity in the POP group, compared

with those in the control group (Fig. 1). Although the number of cases was insufficient to determine whether there was a linear correlation between the severity of oxidative injury and POP staging, the data obtained confirmed the presence of OS in prolapsed USL, which was partially in accordance with previous conclusions (31,32).

In order to determine the exact role of OS in the pathogenesis of POP and the associated mechanisms, it is necessary to establish an OS cell model in fibroblasts derived from USL tissue of non-POP women (hUSLFs). As described above, a series of dose-effect investigations were performed in the present study to determine the appropriate concentration and incubation duration (Figs. 2 and 3). In addition, the rationale of the cell model was verified from two aspects, the generation of intracellular ROS (Fig. 4) and the production of 8-OHdG (Fig. 5). To the best of our knowledge, the present study is the first to successfully establish an OS model in hUSLFs via H_2O_2 incubation, and this cell model may facilitate further investigations involving OS in POP. Due to time and experimental technology constraints, the present study was limited, resulting in examination of the cell model with immunofluorescence only. The addition of Western blot or PCR data is required to provide more systemic and persuasive conclusions.

The primary aim of the present study was to elucidate the effects of OS on collagen metabolism in hUSLFs. The results of the present study revealed that exogenous H_2O_2 had two-way regulatory effects on collagen metabolism (Fig. 6). Following incubation for 24 h, lower concentrations of H_2O_2 stimulated the anabolism of COL1A1, whereas higher concentration promoted catabolism. The specific effect was dependent on the severity of OS. Therefore, it was concluded that OS contributed to collagen metabolic disorder in the human pelvic fibroblasts. To examine the associated mechanisms, MMP-2, TIMP-2 and TGF- β 1 were examined. MMP-2, as a key proteinase responsible for degradation of collagen, has been well demonstrated in previous reports, and TIMP-2 acts as a metalloproteinase inhibitor. According to reports on fibrotic diseases, TGF- β 1, a 25 kDa polypeptide tissue growth factor, has been identified as an important cytokine, which promotes fibrosis by inducing fibroblast differentiation, stimulating synthesis of ECM and inhibiting its degradation. The TGF- β 1/small mothers against decapentaplegic 3 signaling pathway is currently viewed as an important regulator that is widely involved in fibrosis and degenerative fibrotic diseases (33-36). However, TGF- β 1 is rarely discussed in previous reports discussing the pathophysiology of POP. Moalli *et al* (37) reported that exogenous TGF- β 1 stimulates the expression of MMP-2 in human pelvic fibroblasts (32). In the present study, the expression levels of MMP2, TIMP2 and TGF β 1 corresponded to the levels of OS. Although the present study did not verify whether the changes in TGF- β 1 were primary or secondary to COL1A1, MMP-2 or TIMP-2, TGF- β 1 may be involved in collagen metabolic disorder by regulating MMP-2 and/or TIMP-2. Further investigation is warranted, and may further assist in further elucidating the pathophysiology of POP.

Elevated oxidative injury is one of the characteristics of POP, and OS contributes to collagen metabolic disorder in a severity-dependent manner in hUSLFs. The present study

hypothesized that OS may be involved in the pathophysiology of POP, either by inhibiting the anabolism of collagen or, alternatively, by promoting catabolism indirectly through the regulation of TGF- β 1 and proteolytic enzymes, including MMPs. Further investigation is required to improve current understanding of the exact mechanism and to elucidate the pathophysiology of POP, which may be beneficial in preventing or disrupting the progression of POP.

Acknowledgements

The authors would like to thank Xu Xue-Xian, Li Yan-Bo, Cheng Yan-Xiang, Luo Ruo-Yu (Department of Gynecology and Obstetrics, Renmin Hospital of Wuhan University) for specimen biopsy assistance. This study was funded by the National Natural Science Foundation of China (grant nos. H0407-81270684 and H0407-81471442).

References

1. Barber MD and Maher C: Epidemiology and outcome assessment of pelvic organ prolapse. *Int Urogynecol J* 24: 1783-1790, 2013.
2. Olsen AL, Smith VJ, Bergstrom JO, Colling JC and Clark AL: Epidemiology of surgically managed pelvic organ prolapse and urinary incontinence. *Obstet Gynecol* 89: 501-506, 1997.
3. Subak LL, Waetjen LE, van den Eeden S, Thom DH, Vittinghoff E and Brown JS: Cost of pelvic organ prolapse surgery in the United States. *Obstet Gynecol* 98: 646-651, 2001.
4. Merrill RM: Hysterectomy surveillance in the United States, 1997 through 2005. *Med Sci Monit* 14: CR24-CR31, 2008.
5. Weber AM, Buchsbaum GM, Chen B, Clark AL, Damaser MS, Daneshgari F, Davis G, DeLancey J, Kenton K, Weidner AC and Word RA: Basic science and translational research in female pelvic floor disorders: Proceedings of an NIH-sponsored meeting. *Neurourol Urodyn* 23: 288-301, 2004.
6. Jelovsek JE, Maher C and Barber MD: Pelvic organ prolapse. *The Lancet* 369: 1027-1038, 2007.
7. Yiou R, Authier FJ, Gherardi R and Abbou C: Evidence of mitochondrial damage in the levator ani muscle of women with pelvic organ prolapse. *Eur Urol* 55: 1241-1243, 2009.
8. Jackson SR, Avery NC, Tarlton JF, Eckford SD, Abrams P and Bailey AJ: Changes in metabolism of collagen in genitourinary prolapse. *Lancet* 347: 1658-1661, 1996.
9. Klutke J, Ji Q, Campeau J, Starcher B, Felix JC, Stanczyk FZ and Klutke C: Decreased endopelvic fascia elastin content in uterine prolapse. *Acta Obstet Gynecol Scand* 87: 111-115, 2008.
10. Chen B and Yeh J: Alterations in connective tissue metabolism in stress incontinence and prolapse. *J Urol* 186: 1768-1772, 2011.
11. Gabriel B, Watermann D, Hancke K, Gitsch G, Werner M, Tempfer C and zur Hausen A: Increased expression of matrix metalloproteinase 2 in uterosacral ligaments is associated with pelvic organ prolapse. *Int Urogynecol J Pelvic Floor Dysfunct* 17: 478-482, 2006.
12. Strinic T, Vulic M, Tomic S, Capkun V, Stipic I and Alujevic I: Matrix metalloproteinases-1, -2 expression in uterosacral ligaments from women with pelvic organ prolapse. *Maturitas* 64: 132-135, 2009.
13. Takacs P, Nassiri M, Gualtieri M, Candiotti K and Medina CA: Uterosacral ligament smooth muscle cell apoptosis is increased in women with uterine prolapse. *Reprod Sci* 16: 447-452, 2009.
14. Sampson N, Berger P and Zenzmaier C: Redox signaling as a therapeutic target to inhibit myofibroblast activation in degenerative fibrotic disease. *Biomed Res Int* 2014: 1-14, 2014.
15. Fisher GJ, Wang ZQ, Datta SC, Varani J, Kang S and Voorhees JJ: Pathophysiology of premature skin aging induced by ultraviolet light. *N Engl J Med* 337: 1419-1428, 1997.
16. Siwik DA, Pagano PJ and Colucci WS: Oxidative stress regulates collagen synthesis and matrix metalloproteinase activity in cardiac fibroblasts. *Am J Physiol Cell Physiol* 280: C53-C60, e2001.

17. Akhtar K, Broekelmann TJ, Miao M, Keeley FW, Starcher BC, Pierce RA, Mecham RP and Adair-Kirk TL: Oxidative and nitrosative modifications of tropoelastin prevent elastic fiber assembly in vitro. *J Biol Chem* 285: 37396-37404, 2010.
18. World Medical Association: World Medical Association Declaration of Helsinki: Ethical principles for medical research involving human subjects. *JAMA* 318: 2191-2194, 2013.
19. Bump RC, Mattiasson A, Bø K, Brubaker LP, DeLancey JO, Klarskov P, Shull BL and Smith AR: The standardization of terminology of female pelvic organ prolapse and pelvic floor dysfunction. *Am J Obstet Gynecol* 175: 10-17, 1996.
20. Hong S, Li H and Wu D, Li B, Liu C, Guo W, Min J, Hu M, Zhao Y and Yang Q: Oxidative damage to human parametrial ligament fibroblasts induced by mechanical stress. *Mol Med Rep* 12: 5342-5348, 2015.
21. Livak KJ and Schmittgen TD: Analysis of relative gene expression data using real-time quantitative PCR and the $2^{-\Delta\Delta Ct}$ method. *Methods* 25: 402-408, 2001.
22. Harman D: Aging: A theory based on free radical and radiation chemistry. *J Gerontol* 11: 298-300, 1956.
23. DeLancey JO, Kearney R, Chou Q, Speights S and Binno S: The appearance of levator ani muscle abnormalities in magnetic resonance images after vaginal delivery. *Obstet Gynecol* 101: 46-53, 2003.
24. Weidner AC, Jamison MG, Branham V, South MM, Borawski KM and Romero AA: Neuropathic injury to the levator ani occurs in 1 in 4 primiparous women. *Am J Obstet Gynecol* 195: 1851-1856, 2006.
25. Lubowski DZ, Swash M, Nicholls RJ and Henry MM: Increase in pudendal nerve terminal motor latency with defaecation straining. *Br J Surg* 75: 1095-1097, 1988.
26. Spence-Jones C, Kamm MA, Henry MM and Hudson CN: Bowel dysfunction: A pathogenic factor in uterovaginal prolapse and urinary stress incontinence. *Br J Obstet Gynaecol* 101: 147-152, 1994.
27. Pimentel DR, Amin JK, Xiao L, Miller T, Viereck J, Oliver-Krasinski J, Baliga R, Wang J, Siwik DA, Singh K, *et al*: Reactive oxygen species mediate amplitude-dependent hypertrophic and apoptotic responses to mechanical stretch in cardiac myocytes. *Circ Res* 89: 453-460, 2001.
28. Davidovich N, DiPaolo BC, Lawrence GG, Chhour P, Yehya N and Margulies SS: Cyclic stretch-induced oxidative stress increases pulmonary alveolar epithelial permeability. *Am J Respir Cell Mol Biol* 49: 156-164, 2013.
29. Rodríguez AI, Csányi G, Ranayhossaini DJ, Feck DM, Blose KJ, Assatourian L, Vorp DA and Pagano PJ: MEF2B-Nox1 signaling is critical for stretch-induced phenotypic modulation of vascular smooth muscle cells. *Arterioscler Thromb Vasc Biol* 35: 430-438, 2015.
30. Kroese LJ and Scheffer PG: 8-hydroxy-2'-deoxyguanosine and cardiovascular disease: A systematic review. *Curr Atheroscler Rep* 16: 452, 2014.
31. Kim EJ, Chung N, Park SH, Lee KH, Kim SW, Kim JY, Bai SW and Jeon MJ: Involvement of oxidative stress and mitochondrial apoptosis in the pathogenesis of pelvic organ prolapse. *J Urol* 189: 588-594, 2013.
32. Ewies A and Elshafie M: High isoprostane level in cardinal ligament-derived fibroblasts and urine sample of women with uterine prolapse. *BJOG* 116: 126-127; author reply 127-128, 2009.
33. Hinz B: The extracellular matrix and transforming growth factor-beta1: Tale of a strained relationship. *Matrix Biol* 47: 54-65, 2015.
34. Rodríguez-Vita J, Sánchez-Galán E, Santamaría B, Sánchez-López E, Rodríguez-Díez R, Blanco-Colio LM, Egido J, Ortiz A and Ruiz-Ortega M: Essential role of TGF-beta/Smad pathway on statin dependent vascular smooth muscle cell regulation. *PLoS One* 3: e3959, 2008.
35. Gordon KJ and Blobel GC: Role of transforming growth factor-beta superfamily signaling pathways in human disease. *Biochim Biophys Acta* 1782: 197-228, 2008.
36. Yang J, Zheng J, Wu L, Shi M, Zhang H, Wang X, Xia N, Wang D, Liu X, Yao L, *et al*: NDRG2 ameliorates hepatic fibrosis by inhibiting the TGF-β1/Smad pathway and altering the MMP2/TIMP2 ratio in rats. *PLoS One* 6: e27710, 2011.
37. Moalli PA, Klingensmith WL, Meyn LA and Zyczynski HM: Regulation of matrix metalloproteinase expression by estrogen in fibroblasts that are derived from the pelvic floor. *Am J Obstet Gynecol* 187: 72-79, 2002.